

# Hypernuclear structure from $\gamma$ -ray spectroscopy

D.J. Millener<sup>a\*</sup>

<sup>a</sup>Brookhaven National Laboratory, Upton, NY 11973, USA

The energies of p-shell hypernuclear  $\gamma$  rays obtained from recent experiments using the Hyperball at BNL and KEK are used to constrain the YN interaction which enters into shell-model calculations that include both  $\Lambda$  and  $\Sigma$  configurations.

## 1. INTRODUCTION

At the time of HYP2000 in Torino, it was possible to discuss the results from two hypernuclear  $\gamma$ -ray experiments using the Hyperball detector array. The first was KEK E419 in which four  $\gamma$ -ray transitions in  ${}^7_\Lambda\text{Li}$  were observed leading to an accurate identification of three out of four bound excited states of  ${}^7_\Lambda\text{Li}$ , in particular the 692-keV separation of the ground-state doublet [1]. The lifetime of the 2.05-MeV  $5/2^+$  state of  ${}^7_\Lambda\text{Li}$  was also measured and interpreted in terms of a shrinkage in the size of the  ${}^6\text{Li}$  core in  ${}^7_\Lambda\text{Li}$  with respect to the free  ${}^6\text{Li}$  [2]. The second experiment, BNL E930, measured a small energy difference of  $\sim 31$  keV between the  $\sim 3$  MeV  $\gamma$ -ray transitions from the two hypernuclear states based on the lowest  $2^+$  state of the  ${}^8\text{Be}$  core in  ${}^9_\Lambda\text{Be}$  [3].

In terms of the standard phenomenological parametrization of the  $\Lambda\text{N}$  effective interaction, a good fit to  ${}^7_\Lambda\text{Li}$  can be obtained with  $\Delta = 0.48$ ,  $S_\Lambda = -0.01$ ,  $S_N = -0.40$ , and  $T = 0.03$ . Here, the spin-dependence for a  $\Lambda$  in a  $0s$  orbit interacting with a p-shell core is specified by four radial integrals  $\Delta$ ,  $S_\Lambda$ ,  $S_N$ , and  $T$  associated with the operators  $s_N \cdot s_\Lambda$ ,  $l_{N\Lambda} \cdot s_\Lambda$ ,  $l_{N\Lambda} \cdot s_N$ , and  $3(\sigma_N \cdot \hat{r})(\sigma_\Lambda \cdot \hat{r}) - \sigma_N \cdot \sigma_\Lambda$ . For a YNG-type effective interaction, Table 2 of Ref. [4] shows that the radial integrals take somewhat larger values for the heavier p-shell hypernuclei because both the nucleon and  $\Lambda$  orbits become more deeply bound with more confined wave functions despite an  $A^{1/3}$  increase in the radius of the Woods-Saxon potential wells. The substantial value for  $\Delta$  is dictated by the ground-state doublet separation of  ${}^7_\Lambda\text{Li}$ . The value of  $S_N$  is required to bring the excitation energy of the 2.05-MeV  $5/2^+$  state down to its observed value (Table 1 of Ref. [4]) and is also important for the energy of the  $1/2^+; 1$  state. As far as  $S_N$  is concerned there is consistency for the excitation energies of the  $3/2^+$  state in  ${}^{13}_\Lambda\text{C}$  (Table 4 of Ref. [4]) and the excited  $1^-$  states in  ${}^{12}_\Lambda\text{C}$  (Table 5 of Ref. [4]). The values of  $S_\Lambda$  and  $T$  are constrained to be small by the energy separation of the excited-state doublet in  ${}^9_\Lambda\text{Be}$  (Table 3 of Ref. [4]) and also play a modest role in the excitation energy of the  $5/2^+$  state and the  $7/2^+$ ,  $5/2^+$  separation in  ${}^7_\Lambda\text{Li}$ .

In 2001, further ( $K^-$ ,  $\pi^- \gamma$ ) experiments were performed as part of BNL E930 using  ${}^{16}\text{O}$  and  ${}^{10}\text{B}$  targets. The primary purpose of the  ${}^{16}\text{O}$  experiment was to search for  $\sim 6.6$ -

---

\*Work supported by the US Department of Energy under contract no. DE-AC02-98CH10886.

MeV  $\gamma$  rays from the  $\nu p_{3/2}^{-1} \Lambda s_{1/2} 1^-$  state to the  $0^-$  and  $1^-$  members of the  $\nu p_{1/2}^{-1} \Lambda s_{1/2}$  ground-state doublet in order to determine a value for the matrix element of the  $\Lambda N$  tensor interaction which makes a large contribution to the doublet splitting. This experiment was successful, determining that the  $0^-$  state is the ground state and that the doublet separation is 27 keV (see the contributions of Ukai and Tamura). In addition, a strong 2.27-MeV  $\gamma$  ray and several other candidates were seen in  ${}^{15}_{\Lambda}\text{N}$  following proton emission from excited states of  ${}^{16}_{\Lambda}\text{O}$ . The  ${}^{10}\text{B}$  experiment still shows no evidence for the ground-state doublet transition in  ${}^{10}_{\Lambda}\text{B}$ . However,  $\gamma$  rays from  ${}^7_{\Lambda}\text{Li}$  and  ${}^9_{\Lambda}\text{Be}$  that provide new information on these hypernuclei were seen.

Finally, two experiments were performed at KEK in 2002. The first, KEK E509, searched for and saw hypernuclear  $\gamma$  rays following stopped  $K^-$  interactions on  ${}^7\text{Li}$ ,  ${}^9\text{Be}$ ,  ${}^{10}\text{B}$ ,  ${}^{11}\text{B}$ , and  ${}^{12}\text{C}$  targets (see the contributions of Miwa and Tamura). The second, KEK E518, established six  $\gamma$ -ray transitions in  ${}^{11}_{\Lambda}\text{B}$  using the  ${}^{11}\text{B}(\pi^+, K^+\gamma){}^{11}_{\Lambda}\text{B}$  reaction (see the contributions of Miura and Tamura).

In the following sections, we investigate how the new information from experiments with the Hyperball can be understood in terms of shell-model calculations for p-shell hypernuclei. The one new ingredient since HYP2000 is that both  $\Lambda$  and  $\Sigma$  hypernuclear configurations are included so that the explicit effects of  $\Lambda - \Sigma$  coupling are evident, at least for one model of the YN interaction.

## 2. THE EFFECTS OF $\Lambda - \Sigma$ COUPLING

The coupling of the  $\Lambda N$  and  $\Sigma N$  channels is important and it has long been known that  $\Lambda - \Sigma$  coupling makes an important contribution to the spacing of the  $1^+$  and  $0^+$  states of  ${}^4_{\Lambda}\text{H}$  and  ${}^4_{\Lambda}\text{He}$ . Akaishi et al. [5] have given a clear demonstration of this effect using G-matrices calculated for use in the small model space of  $s$  orbits only. The splittings for the NSC97e and NSC97f interactions bracket the observed spacings of the  $1^+$  and  $0^+$  states and it is found that the  $\Lambda N$  spin-spin interaction and the  $\Lambda - \Sigma$  coupling make comparable contributions to the spacing.

To extend this calculation to p-shell hypernuclei, we take the YNG interaction of Akaishi for the  $\Lambda - \Sigma$  coupling and perform shell-model calculations with a basis of  $p^n s_{\Lambda}$  and  $p^n s_{\Sigma}$  configurations. Initially, the  $\langle N\Lambda | G | N\Sigma \rangle$  two-body matrix elements have been computed from the YNG interaction using harmonic oscillator wave functions with  $b = 1.7$  fm. The YNG interaction has non-central components but the dominant feature is a strong central interaction in the  ${}^3S$  channel reflecting the second-order effect of the strong tensor interaction in the  $\Lambda N - \Sigma N$  coupling. Because the relative wave function for a nucleon in a  $p$  orbit and a hyperon in an  $s$  orbit is roughly half  $s$  state and half  $p$  state, the matrix elements coupling  $\Lambda$ -hypernuclear and  $\Sigma$ -hypernuclear configurations are roughly a factor of two smaller than those for the  $A = 4$  system. Because the energy shifts for the  $\Lambda$ -hypernuclear states are given by  $v^2/\Delta E$ , where  $v$  is the coupling matrix element and  $\Delta E \sim 80$  MeV, the shifts in p-shell hypernuclei will be roughly a quarter of those for  $A = 4$  in favorable cases; e.g. 150 keV if the  $\Lambda - \Sigma$  coupling accounts for about half of the  $A = 4$  splitting. For  $T = 0$  hypernuclei, the effect will be smaller because the requirement of a  $T = 1$  nuclear core for the  $\Sigma$ -hypernuclear configurations brings in some recoupling factors which are less than unity.

We note that many interesting new results have been obtained on the effects of  $\Lambda - \Sigma$  coupling in few-body calculations for the s-shell hypernuclei [6–8].

### 3. RESULTS FOR P-SHELL HYPERNUCLEI

We first consider  ${}^7_{\Lambda}\text{Li}$  and  ${}^9_{\Lambda}\text{Be}$  to illustrate some features of the inclusion of  $\Lambda - \Sigma$  coupling. In addition, there is new experimental information on each of these hypernuclei from the BNL E930 run with a  ${}^{10}\text{B}$  target. Then we turn to  ${}^{16}_{\Lambda}\text{O}$  and  ${}^{15}_{\Lambda}\text{N}$  which were studied in the BNL E930 run with a  ${}^{16}\text{O}$  target and finally to  ${}^{11}_{\Lambda}\text{B}$  which was studied in the KEK E518 experiment with a  ${}^{11}\text{B}$  target.

#### 3.1. ${}^7_{\Lambda}\text{Li}$

The  $\Lambda - \Sigma$  coupling matrix elements for a nucleon in the p-shell and a hyperon in the s-shell were calculated for the SC97f(S) effective interaction of Akaishi et al. [5] as described in the preceding section. These matrix elements were multiplied by 0.9 to simulate the  $\Lambda - \Sigma$  coupling of SC97e(S) and thus the observed doublet splitting for  ${}^4_{\Lambda}\text{He}$  (see [5]). In the same parametrization as the  $\Lambda\text{N}$  interaction,

$$\bar{V} = 1.45 \quad \Delta = 3.04 \quad S_{\Lambda} = -0.085 \quad S_{\text{N}} = -0.085 \quad T = 0.157. \quad (1)$$

To reproduce the ground-state doublet splitting of 692 keV for  ${}^7_{\Lambda}\text{Li}$  with  $\Lambda - \Sigma$  coupling included requires a 10% reduction in  $\Delta$  for the  $\Lambda\text{N}$  interaction. A small reduction in the magnitude of  $S_{\text{N}}$  is then required to fit the excitation energy of the  $5/2^+$  state exactly. The contributions to the energy spacings for

$$\Delta = 0.432 \quad S_{\Lambda} = -0.010 \quad S_{\text{N}} = -0.390 \quad T = 0.028 \quad (2)$$

are given in Table 1. The coefficients of the  $\Lambda\text{N}$  interaction parameters are very close to those given in Ref. [4]. The actual energy shifts due to  $\Lambda - \Sigma$  coupling for the  $1/2^+$ ,  $3/2^+$ ,  $5/2^+$  and  $7/2^+$  states with  $T = 0$  are 77, 6, 74, and 0 keV while those for the  $1/2^+$ ,  $3/2^+$ , and  $5/2^+$  states with  $T = 1$  are 97, 101, and 95 keV.

Taking simple LS wave functions for the  ${}^6\text{Li}$  core, one can predict quite well the effects of  $\Lambda - \Sigma$  coupling in the full shell-model calculation. For the ground-state, the only important  $\Sigma$  configuration involves a  $0^+$ ,  $T = 1$  core. The recoupling brings in an extra factor of  $1\sqrt{3}$  in the coefficient before the  ${}^3S$  G-matrix element compared with the  $A = 4$   $0^+$  state. The net effect is an order of magnitude smaller shift than for the  $A = 4$  system.

Table 1

Contributions from  $\Lambda - \Sigma$  coupling and the spin-dependent components of the effective  $\Lambda\text{N}$  interaction to energy spacings in  ${}^7_{\Lambda}\text{Li}$ . Energies are in keV.

Level pair	$\Delta E_{\text{core}}$	$\Lambda\Sigma$	$\Delta$	$S_{\Lambda}$	$S_{\text{N}}$	T	$\Delta E$	Expt.
$3/2^+ - 1/2^+$	0	71	621	-1	-6	-6	690	692
$5/2^+ - 1/2^+$	2186	3	75	11	-272	31	2052	2050
$1/2^+ - 1/2^+$	3565	-20	415	0	-183	-2	3773	3877
$7/2^+ - 5/2^+$	0	74	559	-22	-7	-67	511	470

It is easy to see that the  $\Lambda - \Sigma$  coupling for the  $3/2^+$  member of the ground-state doublet occurs only through the much weaker non-central interactions. Thus,  $\Lambda - \Sigma$  coupling provides only 10% of the ground-state doublet splitting compared with  $\sim 50\%$  for  $A = 4$ . Comprehensive few-body calculations for the  $A = 4$  and  $A = 7$  hypernuclei should be able to put a strong constraint on the overall strength of the  $\Lambda - \Sigma$  coupling in the free YN interaction.

The energy shifts for the doublet based on the  $3^+$  state of the core are similar to those in the ground-state doublet while the energy shifts for the  $T = 1$  hypernuclear states are somewhat larger than for the  $1/2^+$  and  $5/2^+$   $T = 0$  states because the  $\Lambda$  and  $\Sigma$  configurations can have the same  $T = 1$  cores and the  $\Sigma$  configurations can also have  $T = 0$  cores.

One new piece of information on the  ${}^7_\Lambda\text{Li}$  spectrum has been obtained from BNL E930. The 2050-keV  $5/2^+ \rightarrow 1/2^+$   $\gamma$  ray is seen rather strongly from the unbound region of  ${}^{10}_\Lambda\text{B}$  produced in the  ${}^{10}\text{B}(K^-, \pi^-)$  reaction. A  $\gamma$ -ray line at 470 keV is seen in coincidence with the 2050-keV  $\gamma$  ray and has been interpreted as the  $7/2^+ \rightarrow 5/2^+$  transition (Tamura in these proceedings). The calculated energy in Table 1 of 511 keV is somewhat too high and can be accommodated by small increases in the magnitudes of  $S_\Lambda$  and/or  $T$ . Such increases are constrained by the excited-state doublet splitting in  ${}^9_\Lambda\text{Be}$  (see Table 2).

We note that the 692-keV  $3/2^+ \rightarrow 1/2^+$   $\gamma$  ray is also seen in BNL E930 and that the 2050-keV  $5/2^+ \rightarrow 1/2^+$   $\gamma$  ray is seen strongly in KEK E509 via the (stopped  $K^-, \gamma$ ) reaction on  ${}^{10}\text{B}$ .

### 3.2. ${}^9_\Lambda\text{Be}$

The bound-state spectrum for  ${}^9_\Lambda\text{Be}$  is shown in Fig. 1, which also gives the  $\gamma$ -ray energies from a reanalysis of the BNL E930 data [3], for the parameter set

$$\Delta = 0.557 \quad S_\Lambda = -0.013 \quad S_N = -0.549 \quad T = 0.038 . \quad (3)$$

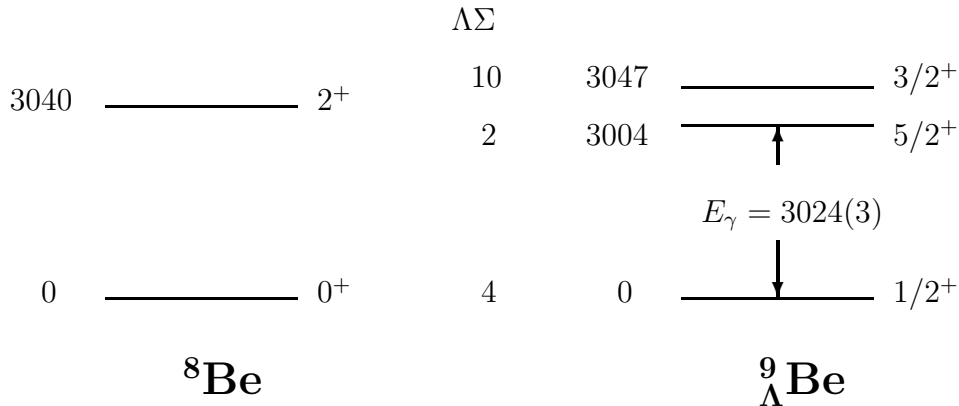


Figure 1. Energy levels of  ${}^9_\Lambda\text{Be}$  and the  ${}^8\text{Be}$  core. The small shifts due to  $\Lambda - \Sigma$  coupling are shown in the center. The measured  $\gamma$ -ray energies are 3024(3) and 3067(3) keV with a separation of 43(5) keV.

Table 2

Contributions from  $\Lambda - \Sigma$  coupling and the spin-dependent components of the effective  $\Lambda N$  interaction to the doublet spacing in  ${}^9_\Lambda\text{Be}$ . Energies are in keV. The spectrum is shown on the right hand side of Fig. 1. The second line gives the coefficients of each  $\Lambda N$  interaction parameter in MeV.

Level pair	$\Delta E_{core}$	$\Lambda\Sigma$	$\Delta$	$S_\Lambda$	$S_N$	T	$\Delta E$
$3/2^+ - 5/2^+$	0	-8	-20	32	-1	38	43
			-0.037	-2.464	0.003	0.994	

The breakdown of the doublet splitting is given in Table 2. As can be seen, the contributions of  $S_\Lambda$  and T work against those from  $\Delta$  and the  $\Lambda - \Sigma$  coupling. Certainly, the value of  $S_\Lambda$  cannot be large. The parameter set chosen puts the  $3/2^+$  state above the  $5/2^+$  state but the order is not determined by this experiment. However, in the 2001 run of BNL E930 on a  ${}^{10}\text{B}$  target, only the upper level is seen following  ${}^{10}_\Lambda\text{B} \rightarrow {}^9_\Lambda\text{Be} + p$ . Then, we can deduce that the  $3/2^+$  state is the upper member of the doublet via the

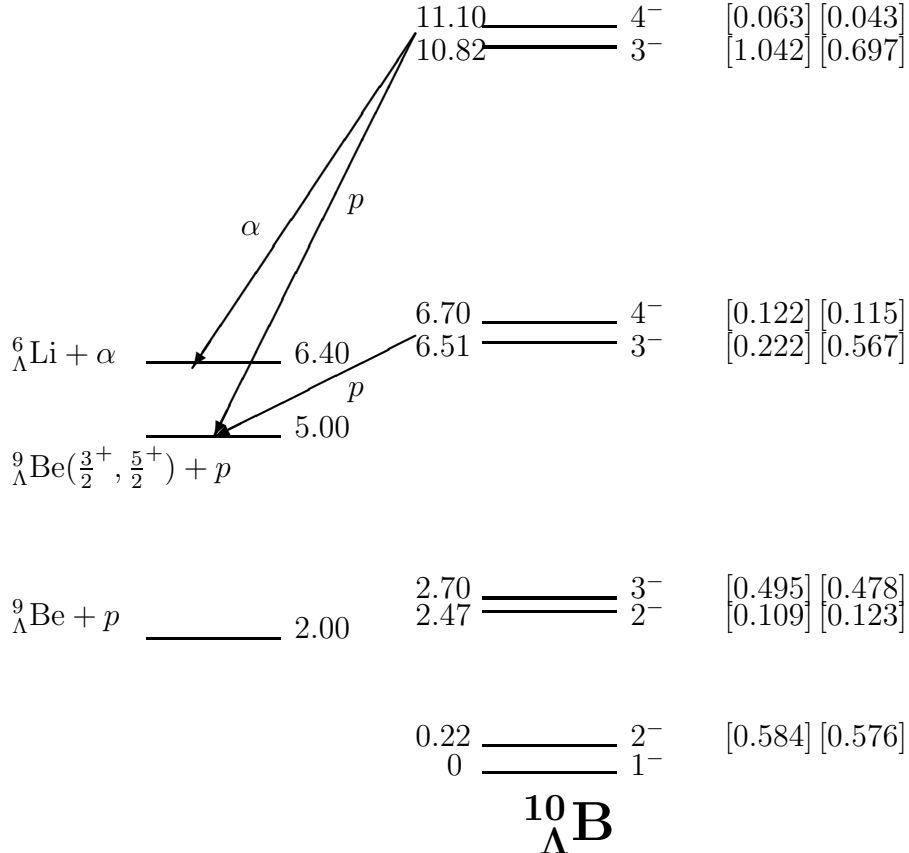


Figure 2. Proton decay of  ${}^{10}_\Lambda\text{B}$  to  ${}^9_\Lambda\text{Be}$ . Formation strengths for non-spin flip production in the  $(K^-, \pi^-)$  reaction are given on the right for two p-shell models. Thresholds for particle decay of the  ${}^{10}_\Lambda\text{B}$  states are given on the left.

following reasoning. Four states of  ${}^9\text{B}$  are reached strongly by neutron removal from  ${}^{10}\text{B}$  [9] and the hypernuclear doublets based on these states are shown in Fig. 2. The structure factors which govern the population of these states are given at the right of the figure for two p-shell interactions. The relative neutron pickup strength to the two  $7/2^-$  states which give rise to the  $3^-/4^-$  doublets above the  ${}^9_\Lambda\text{Be}^* + p$  threshold is very sensitive to the non-central components of the p-shell interaction. Formation of the the  $3^-$  states is favored for the dominant  $p_{3/2}$  removal by the coupling to get  $\Delta L = 1$  and  $\Delta S = 0$ . The proton decay arises from  ${}^9\text{B}(7/2^-) \rightarrow {}^8\text{Be}(2^+) + p$  in the core. The  $4^-$  states proton decay to  ${}^9_\Lambda\text{Be}(5/2^+)$  and from the recoupling  $(2^+ \times p_{3/2})7/2^- \times s_\Lambda \rightarrow (2^+ \times s_\Lambda)J_f \times p_{3/2}$  one finds that the  $3^-$  states proton decay to the  $3/2^+$  and  $5/2^+$  states in the ratio of 32 to 3. Overall, the the  $3/2^+$  state is favored by a factor of more than 3. The only caveat to this argument is that the uppermost  $3^-$  state doesn't  $\alpha$  decay too much.

### 3.3. ${}^{10}_\Lambda\text{B}$

Table 3 shows details of the energy splitting of the ground-state doublet of  ${}^{10}_\Lambda\text{B}$  for the  ${}^7_\Lambda\text{Li}$  parameter set given in Eq. (2). The predicted doublet splitting should be observable but was not seen in an early Brookhaven experiment [10] and is not seen in BNL E930. Theoretically, the splitting is mainly due to the  $\Lambda\text{N}$  spin-spin interaction but does have the interesting feature that the effect of  $\Lambda - \Sigma$  coupling works against the  $\Lambda\text{N}$  spin-spin interaction. This happens because the coupling matrix element to the  ${}^9\text{B}(gs) \times s_\Sigma$  configuration is much larger for the  $2^-$  state than for the  $1^-$  state; in fact, the coupling to the  ${}^9\text{B}(1/2^-) \times s_\Sigma$  state is most important for the  $1^-$  state.

Table 3

Contributions from  $\Lambda - \Sigma$  coupling and the spin-dependent components of the effective  $\Lambda\text{N}$  interaction to energy spacings in  ${}^{10}_\Lambda\text{B}$ . Coefficients (first line) in MeV, energies in keV. The energy shifts due to  $\Lambda - \Sigma$  coupling are 49 and 34 keV for the  $2^-$  and  $1^-$  states.

$\Lambda\Sigma$	$\Delta$	$S_\Lambda$	$S_N$	T	$\Delta E$
	0.579	1.413	0.013	-1.073	
-15	250	-14	-5	-32	180 keV

### 3.4. ${}^{16}_\Lambda\text{O}$

A measurement of the ground-state doublet splitting in  ${}^{16}_\Lambda\text{O}$  has long been desirable because of the strong dependence of the energy separation on the  $\Lambda\text{N}$  tensor interaction. This objective has been achieved in BNL E930 (Ukai and Tamura, these proceedings) by observing the  $\gamma$  rays from the excited  $1^-$  level (see Fig. 3). The measured  $\gamma$ -ray energies and intensities are  $6558.6 \pm 1.4$  keV ( $200 \pm 23$  counts) and  $6532.1 \pm 1.8$  keV ( $128 \pm 20$  counts) for a splitting of  $26.5 \pm 2.3$  keV. Fig. 3 shows the calculated spectrum for the parameter set

$$\Delta = 0.468 \quad S_\Lambda = -0.011 \quad S_N = -0.354 \quad T = 0.030 . \quad (4)$$

Table 4 shows that the dominant contributions to the ground-state doublet splitting are due to  $\Delta$  and T. The rise of the  $\gamma$ -ray energies from the 6176 keV separation of the

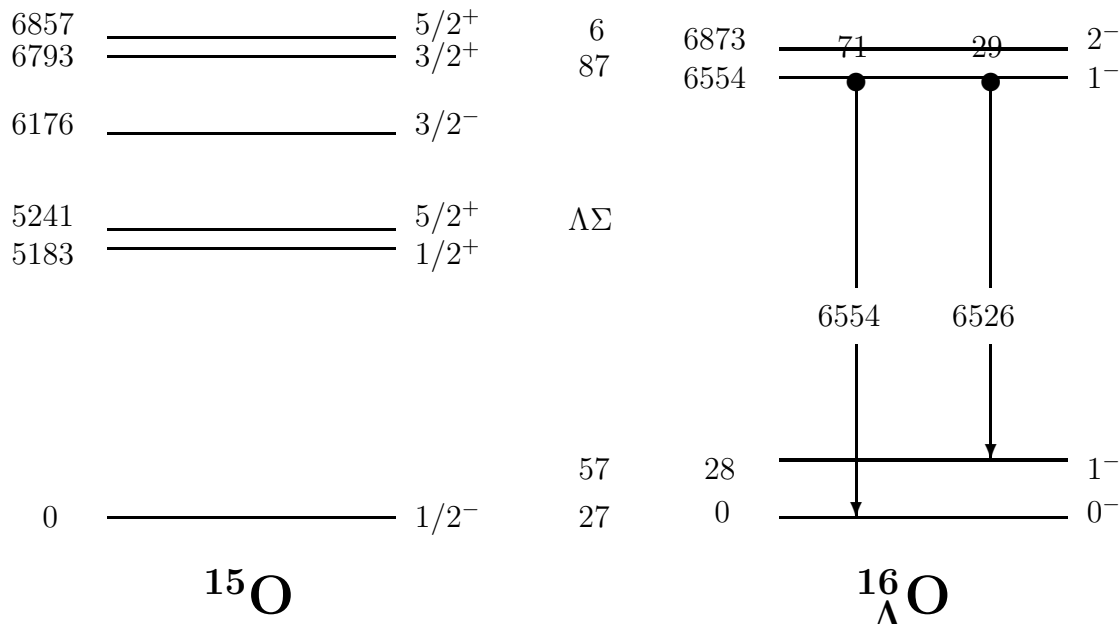


Figure 3. Spectra of  $^{15}\text{O}$  and the  $p^{-1}s_{\Lambda}$  states of  $^{16}_{\Lambda}\text{O}$  for the parameter set of Eq. (4). The energy shifts due to  $\Lambda - \Sigma$  coupling are given in keV.

core levels in  $^{15}\text{O}$  is of course due to  $S_N$  which contributes 530 keV to the separation of the two  $1^-$  levels. The fact that the energy separation between the two lowest peaks in a  $(\pi^+, K^+)$  experiment is  $6.22 \pm 0.06$  MeV [11] suggests that hypernuclear levels based on the lowest positive-parity levels contribute to the cross section.

Table 4

Breakdown of the ground-state doublet splitting for  $^{16}_{\Lambda}\text{O}$ .

$\Lambda\Sigma$	$\Delta$	$S_{\Lambda}$	$S_N$	T	$\Delta E$
	-0.382	1.378	-0.004	7.850	
-30	-179	-15	1	235	28 keV

### 3.5. $^{15}_{\Lambda}\text{N}$

In the  $^{16}\text{O}(K^-, \pi^-)^{16}_{\Lambda}\text{O}$  reaction used for BNL E930,  $p^{-1}p_{\Lambda} 0^+$  states are strongly excited at about 10.6 and 17.0 MeV in excitation energy along with a broad distribution of  $s^{-1}s_{\Lambda}$  strength centered near 25 MeV [12]. These levels can decay by proton emission (the threshold is at  $\sim 7.8$  MeV) to  $^{15}_{\Lambda}\text{N}$  via  $s^4p^{10}(sd)_{s_{\Lambda}}$  components in their wave functions. For example, the wave function of the pure non-spurious component underlying the s-hole strength is

$$|s^{-1}s_{\Lambda}; 0^+\rangle = \sqrt{4/5}s^3p^{12}_{s_{\Lambda}} + \sqrt{1/5}s^4p^{10}(sd)_{s_{\Lambda}}. \quad (5)$$

By setting a cut for small pion angles, where the  $\Delta L = 0$  cross section is large, it was possible to observe  $\gamma$  rays from states of  $^{15}_{\Lambda}\text{N}$  in BNL E930 (Tamura in these proceedings).

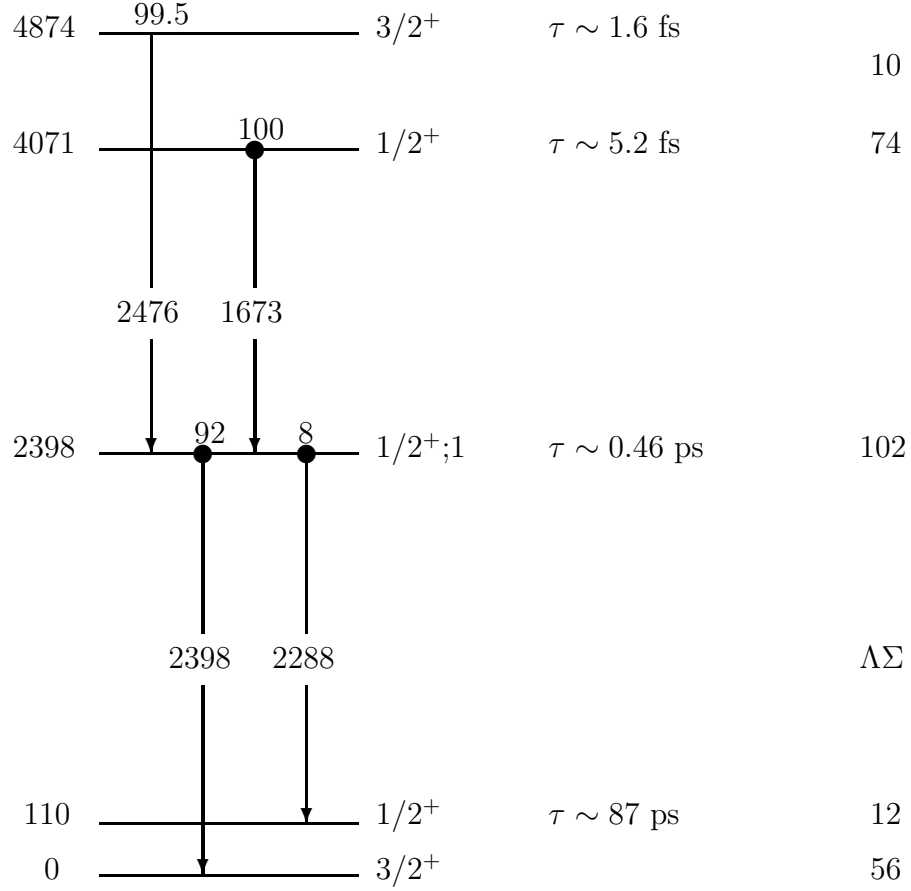


Figure 4. States of  $^{15}_{\Lambda}\text{N}$  based on the  $1^+;0$  ground state, 2313 keV  $0^+;1$  state, and 3948 keV  $1^+;0$  state of the  $^{14}\text{N}$  core for the parameter set of Eq. (4).

The strongest line is observed at 2268 keV in the spectra without Doppler correction. In Fig. 4, this line would be identified with the  $1/2^+;1 \rightarrow 3/2^+$  transition. Note that the ordering of states in the ground-state doublet violates the usual ordering that has the lower-spin state lowest; in the simplest model with  $p_{1/2}$  nucleon holes only, the  $1/2^+$  state would be lowest and the  $^{15}_{\Lambda}\text{N}$  splitting would be 1.5 times that in  $^{16}_{\Lambda}\text{O}$  [13]. As for  $^{16}_{\Lambda}\text{O}$ ,  $\Delta$  and T give large and cancelling contributions to the ground-state doublet splitting. However, because of the deviation of the  $^{14}\text{N}$  ground-state wave function from  $jj$  coupling, the coefficient of  $\Delta$  in Table 5 for  $^{15}_{\Lambda}\text{N}$  is relatively larger than that of T and this leads to the inversion.

Table 5

Breakdown of the ground-state doublet splitting in  $^{15}_{\Lambda}\text{N}$  or the parameter set of Eq. (4).

$\Lambda\Sigma$	$\Delta$	$S_{\Lambda}$	$S_N$	T	$\Delta E$
	0.756	-2.250	0.035	-9.864	
44	354	25	-12	-296	110 keV



In the weak-coupling limit, the B(M1) values for the decay to the  $3/2^+$  and  $1/2^+$  states are in the ratio of 2:1. However, the core M1 transition is very weak and mostly orbital because the  $\langle\sigma\tau\rangle$  matrix element is very small in analogy to  $^{14}\text{C}$   $\beta$  decay. Then, small admixtures of  $1_2^+ \times s_\Lambda$  configurations into the final states produce substantial cancellations

$$\begin{aligned} M(1/2^+; 1 \rightarrow 1/2^+) &= -\{(0.9980)(0.9992)(-0.25496) + (0.0619)(0.9992)(3.21472)\} \\ &= -\{-0.25427 + 0.19883\} = 0.0554, \end{aligned} \quad (6)$$

$$\begin{aligned} M(1/2^+; 1 \rightarrow 3/2^+) &= \{(0.9980)(0.9992)(-0.25496) + (0.0302)(0.9992)(3.21472)\} \\ &= \{-0.25427 + 0.09700\} = -0.1573. \end{aligned} \quad (7)$$

The first numbers in the second product are the admixing amplitudes for the  $1_2^+ \times s_\Lambda$  components while the third numbers in each product are the core M1 matrix elements. The full result for an effective M1 operator which reproduces local p-shell M1 data gives a partial lifetime of 0.5 ps (for  $E_\gamma = 2263$  keV) and the branching ratios shown in Fig. 4. Clearly, the observation of both  $\gamma$ -rays and the comparison with the ground-state doublet splitting of  $^{16}_\Lambda\text{O}$  would be very informative.

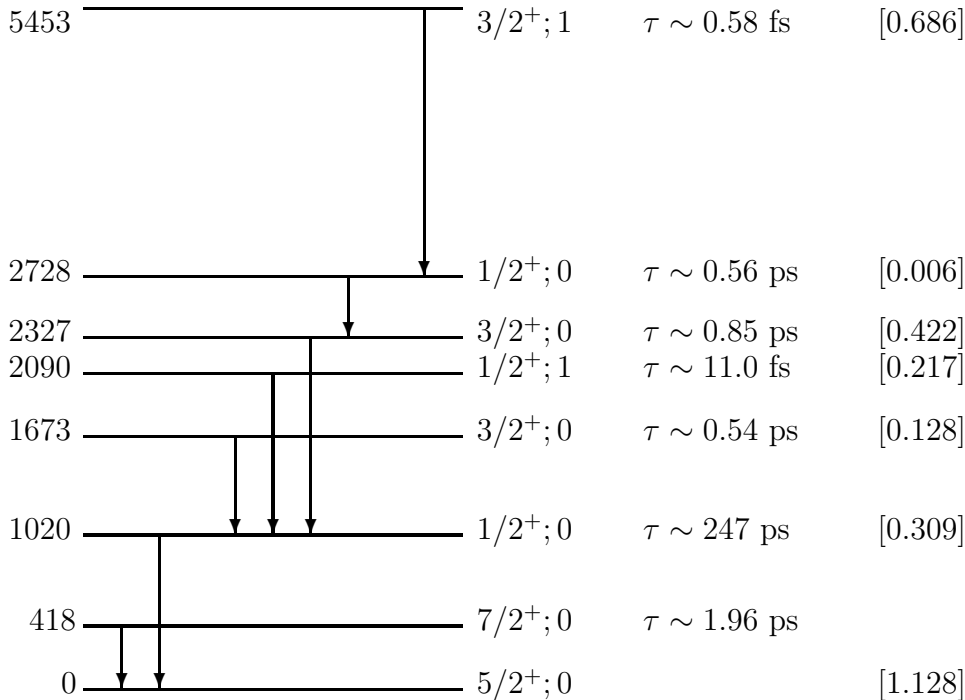


Figure 5. Partial level scheme for  $^{11}_\Lambda\text{B}$  together with calculated lifetimes and formation strengths. The indicated  $\gamma$ -ray transitions are those that are predicted to be strong enough to be seen in KEK E419.

### 3.6. ${}^{11}_{\Lambda}\text{B}$

The  ${}^{10}\text{B}$  core has a number of p-shell levels at low energy and the proton threshold in  ${}^{11}_{\Lambda}\text{B}$  is at 7.72 MeV which leads to a very rich spectrum of  $\gamma$ -ray transitions that potentially provides for many cross checks on the parametrization of the YN interaction. Fig. 5 shows a partial spectrum for  ${}^{11}_{\Lambda}\text{B}$  and gives predictions for  $\gamma$ -rays that might be seen via the  ${}^{11}\text{B}(\pi^+, K^+\gamma){}^{11}_{\Lambda}\text{B}$  reaction used for KEK E518. The Barker I interaction [14] used for the  ${}^{10}\text{B}$  core was chosen to reproduce the empirically optimized wave functions discussed by Kurath [15]. With standard p-shell effective g-factors and charges these wave functions give a good description of electromagnetic transitions in  ${}^{10}\text{B}$ . For the hypernuclear calculation, the formation strengths for each level below the proton threshold were combined with the calculated  $\gamma$ -ray branches to predict the relative intensities of  $\gamma$ -rays produced in the cascade. The lowest  $1/2^+; 0$  level serves as a collection point although for the predicted energy and lifetime in Fig. 5 this level would weak decay more than 50% of the time. In the data, a 1482 keV  $\gamma$  ray is the strongest and five other  $\gamma$ -rays at 262, 454, 500, 564, and 2479 keV are observed with intensities of 9–17% relative the 1482-keV line. At an energy of 1482 keV, the lifetime of the  $1/2^+; 0$  level should be  $\sim 38$  ps and the level should mostly  $\gamma$  decay. The 2479 keV shows up in the Doppler corrected spectrum and it is natural to identify it with the strong M1 transition from the the  $3/2^+; 1$  level to the  $1/2^+; 0$  level. The other four observed transitions are more difficult to place especially in light of the discrepancy between theory and experiment for the  $1/2^+; 0$  level and the fact that the predictions for the  $1/2^+$  and  $3/2^+$  levels based on the  $1^+; 0$  core levels at 718 and 2154 keV are rather volatile with respect to changes in the p-shell interaction.

## 4. CONCLUSION

We are now able to understand considerable body of hypernuclear data in terms of one parametrization of the YN interaction used in shell-model calculations which include  $\Lambda$  and  $\Sigma$  degrees of freedom although the ground-state doublet of  ${}^{10}_{\Lambda}\text{B}$  is still a problem.

## REFERENCES

1. H. Tamura et al., Phys. Rev. Lett. 84 (2000) 5963.
2. K. Tanida et al., Phys. Rev. Lett. 86 (2001) 1982.
3. H. Akikawa et al., Phys. Rev. Lett. 88 (2002) 082501.
4. D.J. Millener, Nucl. Phys. A 691 (2001) 93c.
5. Y. Akaishi, T. Harada, S. Shinmura, and K.S. Myint, Phys. Rev. Lett. 84 (2000) 3539.
6. E. Hiyama et al., Phys. Rev. C 65 (2001) 011301.
7. A. Nogga, H. Kamada, and W. Glöckle, Phys. Rev. Lett. 88 (2002) 172501.
8. H. Nemura, Y. Akaishi, and Y. Suzuki, Phys. Rev. Lett. 89 (2002) 142504.
9. L.A. Kull and E. Kashy, Phys. Rev. 167 (1968) 963.
10. R.E. Chrien et al., Phys. Rev. C 41 (1990) 1062.
11. O. Hashimoto, Nucl. Phys. A 639 (1998) 93c and private communication.
12. W. Brückner et al., Phys. Lett. B 79 (1978) 157.
13. D.J. Millener et al., Phys. Rev. C 31 (1985) 499.
14. F.C. Barker, Aust. J. Phys. 34 (1981) 7.
15. D. Kurath, Nucl. Phys. A317 (1979) 175.